Progress In Electromagnetics Research M, Vol. 96, 45–54, 2020

Dual-Band Rectenna for Wireless Information and Power Transmission of WLAN Applications

Ju Huang, Shixing Yu, Na Kou, Zhao Ding, and Zhengping Zhang*

Abstract—A dual-band microstrip rectenna for wireless local area network (WLAN) applications is presented. It consists of a dual-band dual-polarized receiving antenna and a dual-band high efficiency rectifier. The receiving antenna includes a circular loop, a coplanar waveguide (CPW), and a microstrip line. To minimize mutual interference and ensure high isolation of more than 20 dB between the dual-polarized ports, a CPW is used to produce vertical polarization modes, and the horizontal polarization modes are fed by a microstrip line. The horizontal excitation port is used for information receiving, while the vertical feeding port transfers enough wireless energy for rectifying. A co-simulation of HFSS and ADS is used for analysing the performance of rectenna. Measured results show that it has the −10 dB reflection coefficient bandwidths of 510 MHz (2.39–3.09 GHz) and 920 MHz (5.16–6.08 GHz) for rectifying Port 1, where the isolation between the ports is higher than 25 dB, and the cross polarization is less than −15 dB in two bands. The maximum microwave-direct current (mw-dc) conversion efficiencies of 67.7% and 57.03% at 2.45 GHz and 5.8 GHz are achieved with a 300 Ω load and 16 dBm receiving power.

1. INTRODUCTION

With the development of information technology, a large number of wireless mobile devices have emerged, and the demand for them has also increased. However, the limitation of battery power supply capacity has become the main bottleneck restricting the development of wireless devices [1]. The arrival of the 5G era has brought greater opportunities to the development of the Internet of Things (IoT) devices. In addition, it has made the problem of efficiently powering wireless devices. A very appealing method to supply power for multiple portable electrical devices [2] without using wires and batteries is the wireless power transfer [3]. At present, the most common wireless energy transmission method is electromagnetic induction, and its transfer efficiency can reach 90%. However, the transmission distance is limited to the order of millimeter or centimeter [4]. Microwave Power Transmission (MPT) technology, which is intended to supply high power through free-space, could provide a good solution to settle this distance difficulty. This technology is utilized to supply power to high-altitude aircrafts, wireless sensors, and radio frequency identification [5–9].

Normally, the transmission system will cause a lot of waste of EM energy when receiving data. There are several EM energy sources available around us such as wasted RF signals sources like Wi-Fi router, cordless phone, Bluetooth earpiece, and wireless mouse. Simultaneously, most of these wireless devices resonate at 2.45 GHz and 5.8 GHz. The energy transmitted in radio frequency could be captured by the receiving antenna and then output as DC power by the rectifier circuit. The combination of antenna and rectifier is commonly referred to as rectenna. If the receiving antenna could collect electromagnetic energy while exchanging information, we can greatly improve the EM energy utilization efficiency. Following that, the concept of Simultaneous Wireless Information and Power Transfer (SWIPT) was

Received 27 July 2020, Accepted 25 August 2020, Scheduled 2 September 2020
* Corresponding author: Zhengping Zhang (zpzhang@gzu.edu.cn).
The authors are with the College of Big Data and Information Engineering, Guizhou University, Guiyang 550025, China.

proposed by Varshney, which means that information and energy can be received and utilized at the same time [10]. Following that, a linear-polarized rectenna has been suggested to realize SWIPT usage in [11]. However, it can only transmit information and collect energy at different times. In [12], a dual-polarized H-shaped printed slot antenna designed in WLAN 2.45 GHz is proposed. A compact dual-band dual-polarized loop-slot planar antenna for multiple-input-multiple-output (MIMO) system was presented in [13], which covers WLAN 2.45 GHz band and WiMAX 3.5 GHz band. Both of them are based on a similar principle for creation of odd and even mode in CPW. Moreover, the aperture-coupled dual-polarized antenna operating at 5.8 GHz has been used to realize SWIPT in [14], which explained how to apply dual-polarized antennas to the system and verified the feasibility. The two orthogonal polarized ports can be used to receive information and energy, respectively. Various single-band rectennas for the ISM band (2.45 GHz) have already been investigated in [15–17]. In general, single-band rectifiers can be used to realize high efficiency easily. Most of these single-band rectennas output insufficient voltage and limit their usage for dual-band applications. Thus, dual-band rectifiers are also highly demanded. In addition, a dual-band microstrip rectifier operating at 2.45 GHz and 5.8 GHz was proposed in [18–22]. A dual-band rectenna for energy harvesting applications was proposed in [23], with the maximum RF-DC conversion efficiencies of 63% and 54.8% at 2.45 GHz and 5.8 GHz. However, the rectenna has only one polarized port and cannot transmit information and energy simultaneously.

In this paper, we propose a rectenna for SWIPT usage which is based on a dual-band dual-polarized antenna in conjunction with a dual-band rectifier. The low-profile dual-band dual-polarized slot receiving antenna can operate well at 2.45 GHz and 5.8 GHz, which has high isolation, stable radiation patterns, and low cross polarization. The dual-band rectifier circuit and the antenna are located on a low-cost FR4 substrate for better integration. Meanwhile, the rectifier works well at the two ISM bands (2.45 and 5.8 GHz), with the measured maximum RF-DC conversion efficiencies of 67.7% and 57.03% at 2.45 GHz and 5.8 GHz.

The following content of the paper will be arranged as follows. Section 2 focuses on the design of dual-band dual-polarized receiving antennas and the simulation results. In Section 3, it mainly introduces the design, simulated and measured results of the dual-band rectenna. In Section 4, some conclusions are finally given.

2. RECEIVING ANTENNA DESIGN AND ANALYSIS

We propose a dual-band dual-polarization circular slot receiving antenna, as shown in Figure 1. In order to ensure high SWPIT performance, the two ports of the dual-polarization receiving antenna should minimize mutual interference when receiving energy and information at the same time. This requires improving the isolation of the two ports of the dual-polarized antenna. The antenna is designed on an inexpensive FR4-epoxy substrate with a thickness of 1.6 mm, loss tangent of 0.02, and relative dielectric

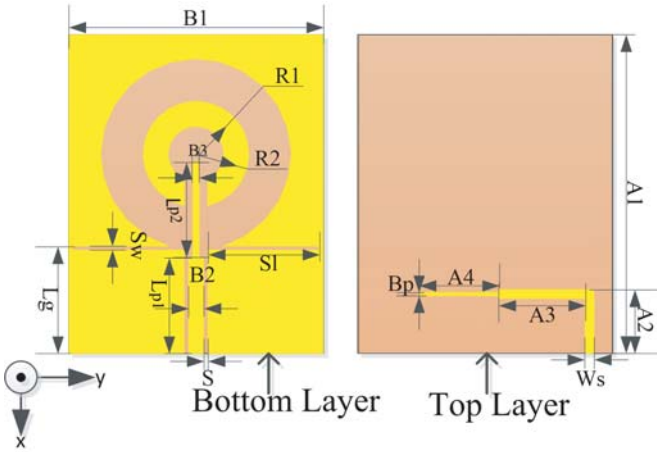

Figure 1. Configuration of the proposed slot antenna.

permittivity of 4.4. Above the substrate is an L-shaped microstrip line, which is fed from Port 2 and excites horizontal polarization. A circular loop and a CPW are designed on the back of the substrate. The CPW connected with the circular loop fed from Port 1 excites vertical polarization. Using two different feeding methods of CPW and microstrip line can improve the isolation and reduce the mutual interference of the two polarized ports. Compared with a similar principle in [12], the dual-polarized antenna in this paper can achieve dual polarizations in two ISM bands.

Two orthogonal polarization ports are used to transmit energy and information respectively. The design process of the receiving antenna is simulated by HFSS software. The final geometrical optimized parameters are shown in Table 1. The resonance frequencies of the vertical polarization mode and horizontal polarization mode are respectively determined by R_1, R_2, and R_3. When Port 1 is fed and Port 2 matched, there is an odd mode in the CPW structure, and the resonant performance is mainly affected by Lp_1 and Lp_2. On the contrary, when the antenna is fed from Port 2, an even mode is excited in the CPW, mainly by adjusting the dimensions of A_2, A_3, A_4, and L_g to make it better match in two bands [13].

Table 1. Geometrical values of the proposed antenna.

Parameter	Value (mm)	Parameter	Value (mm)	Parameter	Value (mm)
B_1	32	B_2	1.93	W_s	1.1
A_1	40	Lp_2	13	A_2	8
L_g	13	B_3	0.8	A_3	12
R_1	24	S	0.54	A_4	11
R_2	13.3	S_l	14	W_p	0.4
Lp_1	12	S_w	0.5		

At 2.45 GHz and 5.8 GHz, when Port 1 is excited, Figure 2(a) shows that the distribution current density is relatively large on both sides of the circular slot loop, mainly concentrated on the CPW and the two vertical edges. At the same time, the direction of current on the upper side of the circular slot loop is opposite, canceled each other out, and the density is small. Receiving antenna produces vertical polarization mode. On the contrary, when Port 1 is matched and Port 2 fed, Figure 2(b) indicates that the current is mainly coupled on the upper edge of the circular slot loop, and the current density on

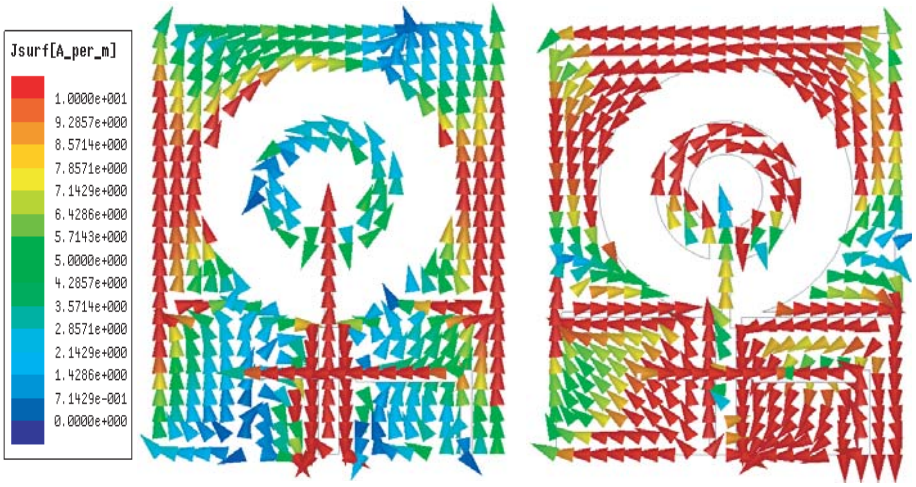

Figure 2. Simulated surface current: fed from (a) Port 1 and (b) Port 2.

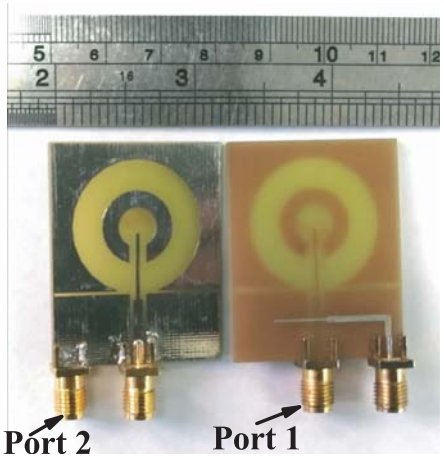

Figure 3. Photograph of the proposed antenna.

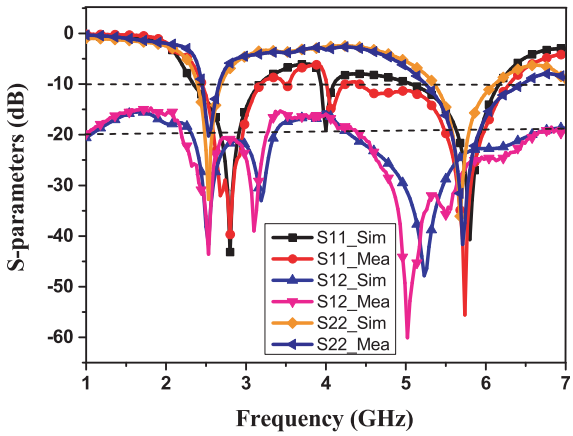

Figure 4. Measured and Simulated S-parameters of the proposed antenna versus frequency.

each side edge is relatively small. Thereby the antenna radiates horizontally polarized fields.

As shown in Figure 3, the proposed antenna was fabricated and measured using the Vector Network Analyzer (VNA) Keysight N5224A. Figure 4 shows the measured and simulated S_{11}-parameters of Port 1, S_{22}-parameter of Port 2, and the isolation S_{21} between two ports. Throughout the ISM (2.45 and 5.8 GHz) bands, the measured results could agree well with simulated effects. In the lower band, the measured results show -10 dB impedance bandwidths of 550 MHz (2.41–2.96 GHz) at Port 1 and 290 MHz (2.39–2.68 GHz) at Port 2. Moreover, the measured isolation is higher than 25 dB, while the lowest values of S_{11} and S_{22} are -25 dB and -40 dB at their resonant frequencies, respectively. In the upper band, the measured -10 dB bandwidth of reflection coefficients S_{11} and S_{22} are 920 MHz and 798 MHz. Simultaneously, the lowest values of S_{11} and S_{22} are -30 dB and -40 dB at their resonant frequencies. Since the receiving antenna and the rectifier circuit designed in the next section are frequency dependent, the frequency offset will cause mismatching, so it is necessary to widen the bandwidth. Hence the stepped feed is introduced to widen the bandwidth of the two bands.

The radiation patterns were measured using a signal generator, a spectrum analyzer, a antenna test turning platform, and horn antennas. Figure 5 and Figure 6 illustrate the measured and simulated radiation patterns of Port 1 and Port 2 at their corresponding resonance bands. As can be seen, the measured and simulated results agree well with each other. Figure 5 shows the H-plane patterns and E-plane patterns of Port 1 at two bands. Figure 6 illustrates the patterns of Port 2 at their resonance frequencies. For Port 1, the vertical polarization is the dominant polarization, and the horizontal polarization is the cross polarization. Moreover, when Port 1 is matched, the horizontal polarization is the dominant polarization. It is seen from the figures that the antenna has low cross polarization. The patterns for E-plane of two ports at both bands exhibit quasi-8 shapes. In addition, the H-plane patterns present omnidirectional characteristics at both bands. The maximum measured gains are observed to be higher than 2.66 dB and 3.16 dB for Ports 1 and 2 in the lower band. In the upper band, the maximum gains of the vertical polarization and horizontal polarization are 4.71 dB and 5.31 dB at their central frequencies.

3. THE RECTENNA DESIGN AND MEASUREMENT

3.1. Rectifier Design

In this part, we propose a dual-band rectifier consisting of a matching network and a dc-pass filter, as shown in Figure 7. The design and performance of the rectifier are analyzed using harmonic balance simulation in Advanced Design System (ADS). The rectifier using microstrip lines is located on the FR4 substrate, which is the same as antenna. The final physical dimensions are shown in Table 2. The topology matching network and the choice of diode determine the overall efficiency of the rectifier.

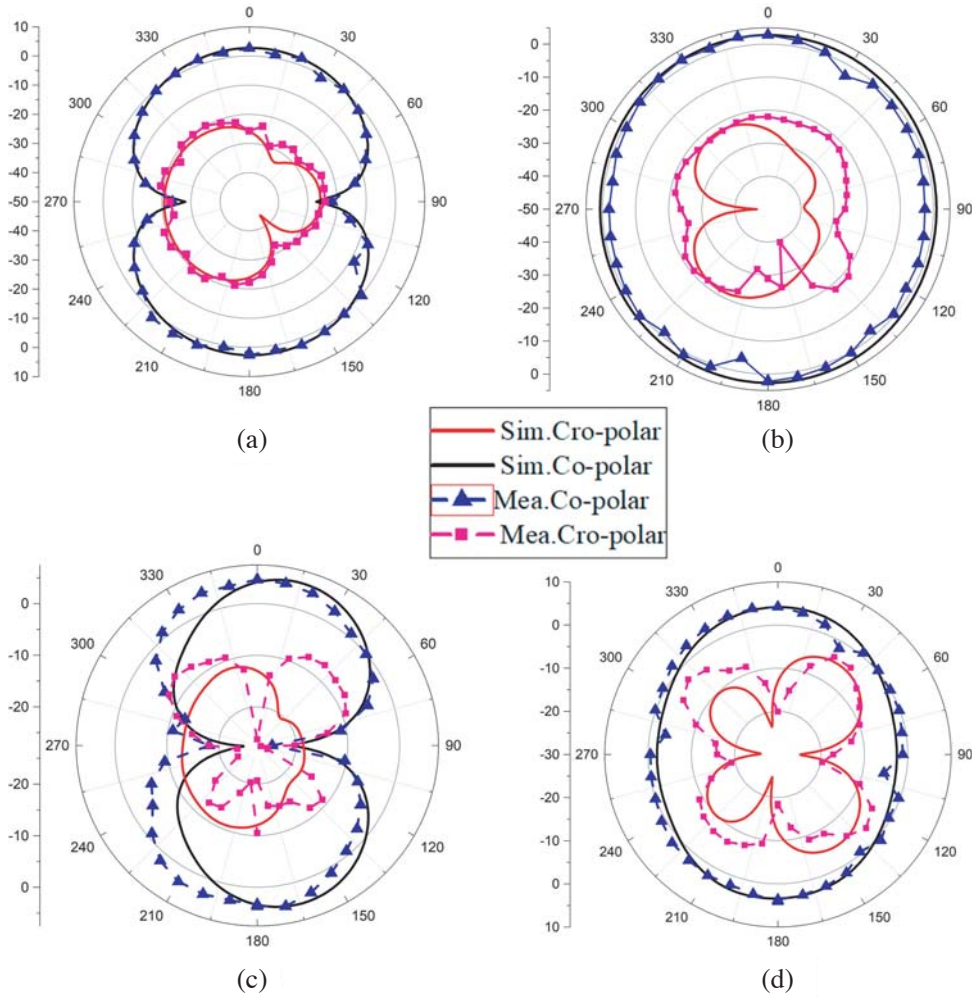

Figure 5. Measured and simulated radiation patterns for Port 1. (a) 2.45 GHz, xz-plane. (b) 2.45 GHz, yz-plane. (c) 5.8 GHz, xz-plane. (d) 5.8 GHz, yz-plane.

Table 2. Geometrical values of the proposed rectifier.

Parameter	Value (mm)	Parameter	Value (mm)	Parameter	Value (mm)
W_1	3	L_3	26.6	W_6	3.7
L_1	5.5	W_4	0.55	L_6	20.3
W_2	0.7	L_4	10.1	W_7	3.2
L_2	27.1	W_5	2.6	L_7	4.85
W_3	0.6	L_5	14.5		

The π-shaped topology is introduced to the network for realizing accurate impedance matching at both bands simultaneously. Moreover, a packaged Schottky diode HSMS2860 is adopted with built-in turn-on voltage $V_{bi} = 0.3\,\text{V}$ and the breakdown voltage $V_B = 7\,\text{V}$ in the circuit.

Figure 8 shows the simulated reflection coefficient versus two operating frequencies. As can be seen, the lowest values of S_{11}-parameters are $-30\,\text{dB}$ and $-40\,\text{dB}$ at 2.45 GHz and 5.8 GHz when the optimal input power is 16 dBm, and the load is $300\,\Omega$.

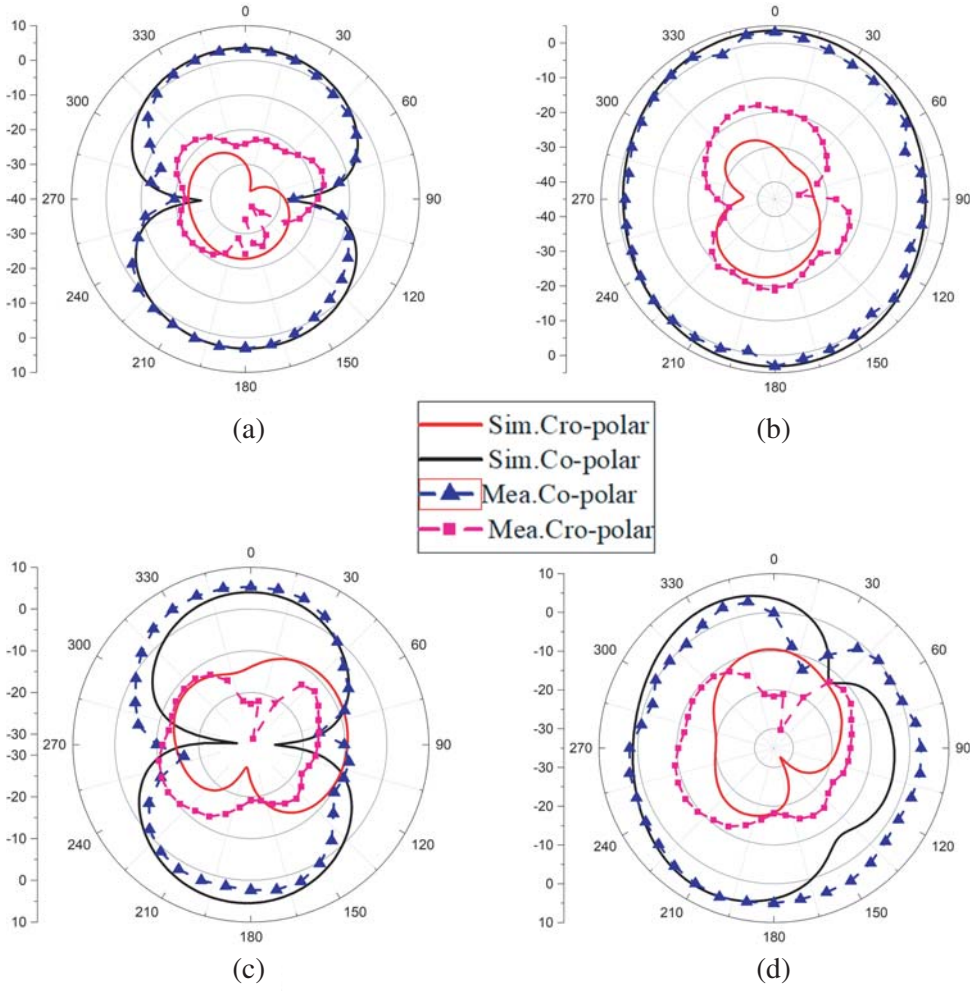

Figure 6. Measured and simulated radiation patterns for Port 2. (a) 2.45 GHz, yz-plane. (b) 2.45 GHz, xz-plane. (c) 5.8 GHz, yz-plane. (d) 5.8 GHz, xz-plane.

3.2. Rectenna Measurement

To validate the performance, the rectifier working at 2.45 GHz and 5.8 GHz is fabricated and tested. Photographs of the rectenna and the measurement setup are illustrated in Figure 9. The vertical polarization port is used for rectifying, as shown in Figure 9(a). Actually, the rectenna can also use its vertical polarization port for information receiving and horizontal polarization port for rectifying. We display the first measurement strategy. The antenna and rectifier were connected by an SMA connector for testing purpose. The conversion efficiency can be calculated according to the following formula:

$$\eta_r = \frac{(V_{load})^2}{R_{load}} * \frac{1}{P_{in}} * 100\% \tag{1}$$

where V_{load} and P_{in} are the output dc voltage across the load resistance and the input power. As can be observed, the input power is obtained by Keysight N5183B. Moreover, the output DC voltage (V_{load}) is measured by a voltage meter. The simulated and measured rectifying efficiencies with corresponding output voltage variation as a function of different input powers are shown in Figure 10. The different input powers are obtained by changing the output power of the signal generator. From Figure 10, the conversion efficiency and output voltage improve as the input power increases. The maximum simulation values of 70.2% (at 2.4 GHz) and 61% (at 5.8 GHz) are observed across a 300 Ω load under the optimal input power of 16 dBm, while the measured peak efficiencies are 67.7% (at 2.45 GHz) and 56.2% (at

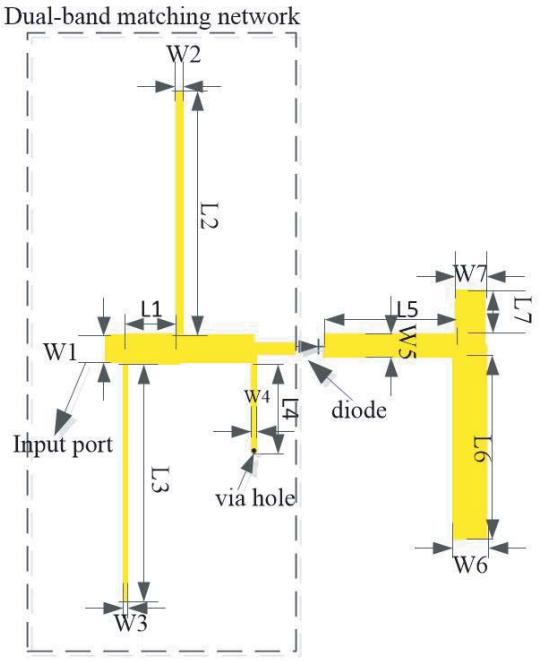

Figure 7. Schematic of the rectifier circuit.

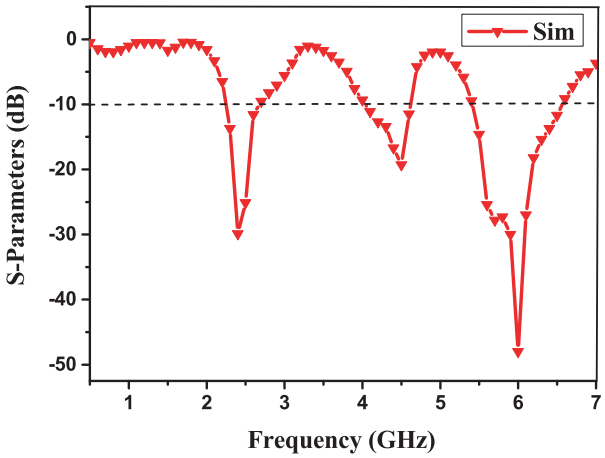

Figure 8. Reflection coefficient versus frequency at the input power of 16 dBm.

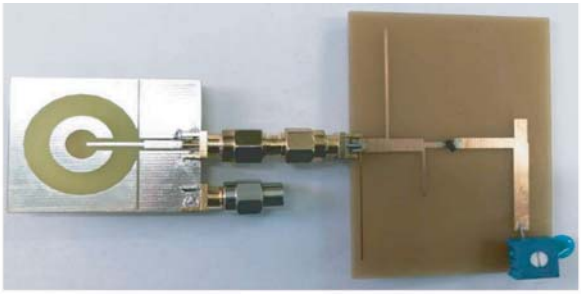

(a)

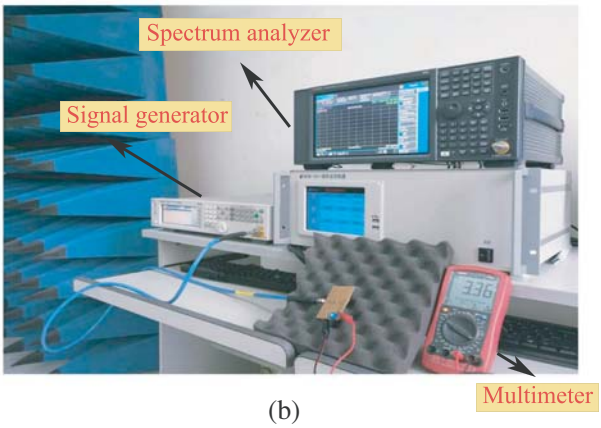

(b)

Figure 9. Photograph of (a) the rectenna and (b) experimental setup.

5.8 GHz). However, there is a negligible increment in output voltage after achieving its maximum value. The reason for this phenomenon is that the rectifying diode will be saturated at a certain input power. Simultaneously, the output voltage is increased to be close to the breakdown voltage. Then, the efficiency decreases sharply with the input power after the optimal value. Figure 10 shows that the efficiency is higher than 50% with the input power range of 7 to 20 dBm at 2.45 GHz. In addition, the efficiency is more than 50% with the range of 9 to 19 dBm at 5.8 GHz. This shows the rectenna is less sensitive in this range of input power values. It can also be noted that the maximum efficiency obtained at 2.45 GHz is higher than that at 5.8 GHz. The reason is that the rectifier leads to more energy loss at 5.8 GHz than that at 2.45 GHz. To obtain the optimal value of the load, a Rheostat was selected to facilitate the experiment. Figure 11(a) shows that the rectifying efficiency increases with the load and reaches its peak values of 67.4% (at 2.4 GHz) and 56.8% (at 5.8 GHz) when the load is 300 Ω, then it gradually decreases.

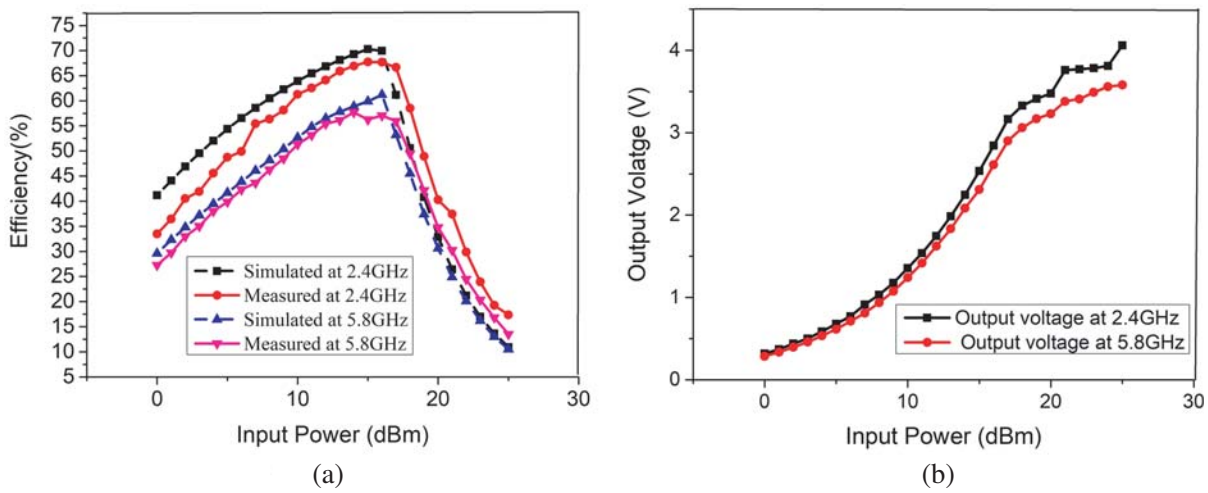

Figure 10. Measured efficiency and output voltage as a function of input power at 2.45 GHz and 5.8 GHz. (a) Conversion efficiency. (b) Output voltage.

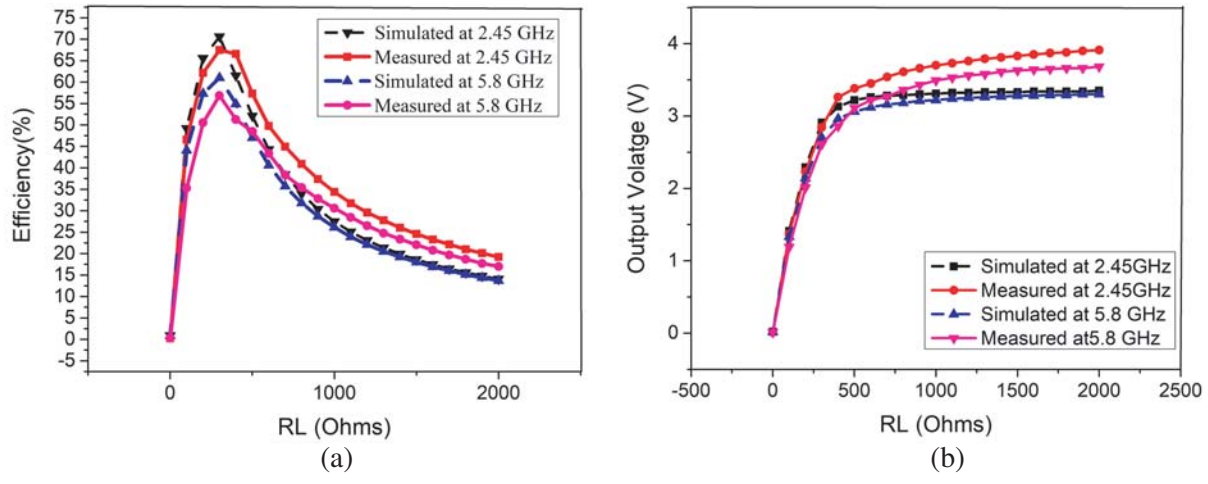

Figure 11. Simulated and measured conversion efficiency with corresponding output voltage versus the load at 2.45 GHz and 5.8 GHz. (a) Conversion efficiency. (b) Output voltage.

4. CONCLUSION

A novel dual-band loop-slot microstrip rectenna for SWIPT usage is proposed in this paper. The prototype is fabricated and measured. By introducing two different feeding structures of CPW and microstrip line, the receiving antenna improves the port isolation and reduces the mutual interference of the two polarized ports. Measured results show that the isolation is higher than 25 dB, and the cross polarization is less than −15 dB in two bands. The step-feed can expand the bandwidth of the receiving antenna when legitimately arranging the ratio of the width and length of the feedline. −10 dB reflection coefficient bandwidths of 510 MHz (2.39–3.09 GHz) and 920 MHz (5.16–6.08 GHz) are measured at the rectifying Port 1. By applying the π-shaped topology, the rectifier can realize accurate impedance matching at both bands. At 2.45 GHz and 5.8 GHz, the rectenna shows that the maximum measured efficiencies are 67.7% and 57.03% under the conditions of 300 Ω load and 16 dBm input power. The dual-band dual-polarized trait, compact size, low cost, and high port isolation are the key advantages of the proposed rectenna. The rectenna can harvest energy sources available around us such as wasted RF signals sources like Wi-Fi router, cordless phone, Bluetooth earpiece, and wireless mouse. Even though the harvesting power is small, it is adequate for various low-power devices such as RFID tags, wireless sensors, and smartwatch. In addition, it can also transfer information between them. With these good performances, the rectenna can be a good candidate for low-power WLAN applications.

ACKNOWLEDGMENT

This work was supported in part by the National Natural Science Foundation of China under Grant 61961006, in part by the Science and Technology Projects of Guizhou Province under Grant QKHJC [2020]1Y256 and [2020]1Y257, and in part by the Central Government Guide to Local Science and Technology Development Fund under Grant QKZYD[2018]4009.

REFERENCES

1. Haboubi, W., H. Takhedmit, J.-D. Lan Sun Luk, S.-E. Adami, B. Allard, F. Costa, C. Vollaire, O. Picon, and L. Cirio, "An efficient dual-circularly polarized rectenna for RF energy harvesting in the 2.45 GHz ISM band," *Progress In Electromagnetics Research*, Vol. 148, 31–39, 2014.
2. Sakamoto, T., Y. Ushijima, E. Nishiyama, M. Aikawa, and I. Toyoda, "5.8-GHz series/parallel connected rectenna array using expandable differential rectenna units," *IEEE Transactions on Antennas and Propagation*, Vol. 61, No. 9, 4872–4875, 2013.
3. Huang, K. and V. K. N. Lau, "Enabling wireless power transfer in cellular networks: Architecture, modeling and deployment," *IEEE Transactions on Wireless Communications*, Vol. 13, No. 2, 902–912, 2014.
4. Xu, D. and Q. Li, "Joint power control and time allocation for wireless powered underlay cognitive radio networks," *IEEE Transactions on Wireless Communications*, Vol. 6, No. 3, 294–297, 2017.
5. Brown, W. C., "The history of power transmission by radio waves," *IEEE Transactions on Microwave Theory and Techniques*, Vol. 32, No. 9, 1230–1242, 1984.
6. Liou, C., C. Kuo, and S. Mao, "Wireless-power-transfer system using near-field capacitively coupled resonators," *IEEE Transactions on Circuits and Systems II: Express Briefs*, Vol. 63, No. 9, 898–902, 2016.
7. Lai, C., et al, "Highly efficient microwave power system of magnetrons utilizing frequency-searching injection-locking technique with no phase shifter," *IEEE Transactions on Microwave Theory and Techniques*, Vol. 63, No. 9, 898–902, 2020.
8. Strassner, B. and K. Chang, "Microwave power transmission: Historical milestones and system components," *Proceedings of the IEEE*, Vol. 101, No. 6, 1379–1396, 2013.
9. Kim, Y., H. S. Bhamra, J. Joseph, and P. P. Irazoqui, "An ultra-low-power RF energy-harvesting transceiver for multiple-node sensor application," *IEEE Transactions on Circuits and Systems II: Express Briefs*, Vol. 62, No. 11, 1028–1032, 2015.

10. Varshney, L. R., "Transporting information and energy simultaneously," *2008 IEEE International Symposium on Information Theory*, No. 6, 1612–1616, 2008.
11. Huang, F., C. Lee, C. Chang, L. Chen, T. Yo, and C. Luo, "Rectenna application of miniaturized implantable antenna design for triple-band biotelemetry communication," *IEEE Transactions on Antennas and Propagation*, Vol. 59, No. 7, 2646–2653, 2011.
12. Li, W., Z. Xia, B. You, Y. Liu, and Q. H. Liu, "Dual-polarized H-shaped printed slot antenna," *IEEE Antennas and Wireless Propagation Letters*, Vol. 16, 1484–1487, 2017.
13. Tan, M. and B. Wang, "A compact dual-band dual-polarized loop-slot planar antenna," *IEEE Antennas and Wireless Propagation Letters*, Vol. 14, 1742–1745, 2015.
14. Yang, X., C. Jiang, A. Z. Elsherbeni, F. Yang, and Y. Wang, "A novel compact printed rectenna for data communication systems," *IEEE Transactions on Antennas and Propagation*, Vol. 61, No. 5, 2532–2539, 2013.
15. Riviere, J., A. Douyere, S. Oree, and J.-D. Lan Sun Luk, "An ISM band conventional CPW rectenna for low power levels," *Progress In Electromagnetics Research C*, Vol. 77, 101–110, 2017.
16. Kharrat, I., P. Xavier, T.-P. Vuong, and G. E. P. Tourtollet, "Compact rectenna design for lossy paper substrate at 2.45 GHz," *Progress In Electromagnetics Research C*, Vol. 62, 61–70, 2016.
17. Monti, G., L. Corchia, and L. Tarricone, "ISM band rectenna using a ring loaded monopole," *Progress In Electromagnetics Research C*, Vol. 33, 1–15, 2012.
18. Ur Rehman, M., W. Ahmad, and W. T. Khan, "Single- and dual-band RF rectifiers with extended input power range using automatic impedance transforming," *IEEE Transactions on Microwave Theory and Techniques*, Vol. 25, No. 5, 1974–1984, 2019.
19. Liu, Z., Z. Zhong, and Y. Guo, "Enhanced dual-band ambient RF energy harvesting with ultra-wide power range," *IEEE Microwave and Wireless Components Letters*, Vol. 25, No. 9, 630–632, 2015.
20. Takhedmit, H., Z. Saddi, and L. Cirio, "A high-performance circularly-polarized rectenna for wireless energy harvesting at 1.85 and 2.45 GHz frequency bands," *Progress In Electromagnetics Research C*, Vol. 79, 89–100, 2017.
21. Li, C., M. Yu, and H. Lin, "A compact 0.9-/2.6-GHz dual-band RF energy harvester using SiP technique," *IEEE Microwave and Wireless Components Letters*, Vol. 27, No. 7, 666–668, 2017.
22. Niotaki, K., A. Georgiadis, A. Collado, and J. S. Vardakas, "Dual-band resistance compression networks for improved rectifier performance," *IEEE Transactions on Microwave Theory and Techniques*, Vol. 62, No. 12, 3512–3521, 2014.
23. Bhatt, K., S. Kumar, P. Kumar, and C. C. Tripathi, "Highly efficient 2.4 and 5.8 GHz dual-band rectenna for energy harvesting applications," *IEEE Antennas and Wireless Propagation Letters*, Vol. 18, No. 12, 2637–2641, 2019.